The Preparation and Preliminary Characterisation of Three Synthetic Andesite Reference Glass Materials (ARM-1, ARM-2, ARM-3) for *In Situ* Microanalysis

Shitou **Wu** (1, 2)* iD, Gerhard **Wörner** (2), Klaus Peter **Jochum** (3) iD, Brigitte **Stoll** (3), Klaus **Simon** (2) and Andreas **Kronz** (2)

(1) Institute of Geology and Geophysics, Chinese Academy of Sciences, Beijing,100029, China
(2) Geowissenschaftliches Zentrum, Göttingen Universität, Göttingen, 37077, Germany
(3) Abteilung für Klimageochemie, Max-Planck-Institut für Chemie, Postfach 3060, D-55020, Mainz, Germany
* Corresponding author. e-mail: shitou.wu@mail.iggcas.ac.cn

Three synthetic reference glasses were prepared by directly fusing and stirring 3.8 kg of high-purity oxide powders to provide reference materials for microanalytical work. These glasses have andesitic major compositions and are doped with fifty-four trace elements in nearly identical abundance (500, 50, 5 $\mu g\ g^{-1}$) using oxide powders or element solutions, and are named ARM-1, 2 and 3, respectively. We further document that sector-field (SF) ICP-MS (Element 2 or Element XR) is capable of sweeping seventy-seven isotopes (from ^7Li to ^{238}U, a total of sixty-eight elements) in 1 s and, thus, is able to quantify up to sixty-eight elements by laser sampling. Micro- and bulk analyses indicate that the glasses are homogeneous with respect to major and trace elements. This paper provides preliminary data for the ARM glasses using a variety of analytical techniques (EPMA, XRF, ICP-OES, ICP-MS, LA-Q-ICP-MS and LA-SF-ICP-MS) performed in ten laboratories. Discrepancies in the data of V, Cr, Ni and Tl exist, mainly caused by analytical limitations. Preliminary reference and information values for fifty-six elements were calculated with uncertainties [2 relative standard error (RSE)] estimated in the range of 1–20%.

Keywords: glass reference materials, microanalysis, sector-field ICP-MS, LA-ICP-MS, multiple-element quantification.

Received 27 Dec 18 – Accepted 18 Sep 19

Precise and accurate chemical determination of trace element abundances in rocks and their mineral constituents provides valuable information concerning element distribution, geochemical processes of element transport, and the compositional evolution of rocks, sediments and soils (Hofmann 2003, Rudnick and Gao 2003). Most analytical data of this sort have been obtained via acid digestion of these materials and subsequent measurement by inductively coupled plasma-optical emission spectroscopy (ICP-OES) and inductively coupled plasma-mass spectroscopy (ICP-MS; e.g., Jenner *et al.* 1990). For the most precise analyses of bulk materials, isotope dilution techniques have been used (e.g., Raczek *et al.* 2001, Willbold *et al.* 2003). However, acid digestion techniques are laborious and do not yield information regarding individual mineral grains and their spatial compositional variation. Since the first demonstration that a laser ablation system could be coupled to an ICP-MS

for *in situ* chemical analysis (Gray 1985), further developments over past 30 years have improved the capabilities of laser ablation systems (Sylvester and Jackson 2016). The wavelength switch from visible/infrared (693 nm ruby, 1064 nm Nd:YAG) to ultraviolet (213 nm Nd:YAG, 193 nm ArF Excimer) has resulted in improved laser absorbance for most targets and produced aerosols with only a small fraction of particles too large to be vaporised in the ICP (Guillong *et al.* 2003). Nowadays, laser ablation ICP-MS is widely accepted as a routine technique for *in situ* and bulk chemical determination in geological samples (Sylvester and Jackson 2016).

The majority of ICP-MS systems used for laser ablation employ a quadruple (Q) mass spectrometer (Jackson *et al.* 1992, Fryer *et al.* 1995, Eggins *et al.* 1998, Jeffries *et al.* 1998, Gao *et al.* 2002, Liu *et al.* 2008, Jenner and O'Neill

2012, Garbe-Schönberg and Müller 2014, He *et al.* 2016, Peters and Pettke 2017) mainly because of its capability to rapidly scan across a large mass range. Compared with the Q-ICP-MS, the sensitivity of sector-field (SF) ICP-MS is higher by a factor of 3–5 (Agilent 7900 vs Element XR), but mass scans are slower. The development of SF-ICP-MS has enabled ultra-trace element determinations at high spatial resolution together with low sample consumption (Latkoczy and Günther 2002). Recently, Wu *et al.* (2018a) documented that the sensitivity of LA-SF-ICP-MS can be further enhanced with the use of a 'Jet Interface' and the addition of small amounts of N_2, allowing ultra-trace element measurements (sub-ng g^{-1} level) in geological samples. However, the magnet settling time of the sector-field mass spectrometer cannot be avoided, leading to a slower mass scan speed, in particular for across a wide mass range (e.g., ^{7}Li to ^{238}U) even though LA-SF-ICP-MS was routinely used for multiple-element quantification with reduced sampling time and/or reduced mass range (Ødegård and Hamester 1997, Flem *et al.* 2002, Latkoczy and Günther 2002, Tiepolo *et al.* 2003, Jochum *et al.* 2007, 2012, Regnery *et al.* 2010, Kimura and Chang 2012, Walle and Heinrich 2014).

Reference glass materials play an important role in laser ablation ICP-MS to ensure measurement precision and accuracy (Jochum and Enzweiler 2014). Such reference materials are commonly used for calibration, quality control and for inter-laboratory comparison of analytical data from different laboratories. Currently, about twenty reference glasses are available for microanalysis, provided and tested mainly by NIST, MPI, USGS and the National Research Centre for Geoanalysis, China (NRCG; Jochum and Enzweiler 2014). The most widely used reference materials are synthetic NIST SRM 610 and NIST SRM 612 glasses in which the mass fractions are high enough for nearly all trace elements (*ca.* 450 µg g^{-1} and *ca.* 40 µg g^{-1}, respectively) for precise calibration. However, the major element compositions of synthetic NIST glasses are very different from that of any geological matrix. This may lead to analytical problems due to matrix effects, in particular for volatile and siderophile/chalcophile elements (e.g., Zn, Cu, Pb; Jochum *et al.* 2014). Therefore, reference glasses closer in major element compositions to natural materials were developed (e.g., USGS BCR-2G, BIR-1G, BHVO-2G and MPI-DING glasses). These are now commonly used only for quality control because of the very low mass fraction of some elements that could result in imprecise calibration. The USGS prepared four synthetic reference glasses with a basaltic major element composition containing many elements in similar abundances at different mass fraction levels (500, 50, 5, 0.01 µg g^{-1}; Jochum *et al.* 2005). To further provide and establish new reference glasses that are close in composition

to natural rocks, we prepared three new synthetic andesite reference glasses by directly fusing and stirring high-purity oxide powders. Each of the produced glass materials has a mass of 3.0 kg doped with fifty-four trace elements at different mass fraction levels of 500, 50 and 5 µg g^{-1}. These glasses are referred to as Andesite Reference Glass Materials (ARM)-1, 2 and 3, respectively.

In this paper, we describe the preparation procedure and provide preliminary mass fraction data for the ARM glasses using a variety of analytical techniques (EPMA, XRF, ICP-OES, ICP-MS, LA-Q-ICP-MS and LA-SF-ICP-MS) performed in different laboratories. The ARM-1, ARM-2, ARM-3 glasses can serve as an alternative to NIST and USGS GS reference glasses for calibration of *in situ* analytical techniques. We further document an acquisition method for the Thermo Element 2 and Element XR SF-ICP-MS instrument that is capable of sweeping seventy-seven isotopes (from ^{7}Li to ^{238}U, a total of sixty-eight elements) in only 1 s. The acquisition efficiency is around 77%, which is four-fifths to that of Q-ICP-MS (acquisition efficiency: 85%). The long-term reproducibility and accuracy of this acquisition method were validated by measurement data of reference materials from NIST, MPI-DING, USGS and NRCG.

Experimental

Preparation of ARM glasses

The ARM glasses were made by fusing and stirring high-purity oxide powders in proportions of an andesite major element composition. The starting material was doped with fifty-four trace elements using oxide powders in similar abundance (500, 50 and 5 µg g^{-1}, respectively); only for Th and U we used element solutions (see details in Appendix S1, Table S1). Considering that the abundance of Ba is higher compared with other trace elements (e.g., REEs) in most natural geological samples, the amounts of Ba added in the three glasses were increased by a factor of ~ 4. Due to the limited amount of element solution, the values of Th and U are significantly lower than other trace elements, especially for ARM-1 and ARM-2.

The glasses were prepared at the China Building Materials Academy, China, by a procedure outlined in Figure 1. Briefly, a total of 3.8 kg mixed oxide powders in a designed proportion were fused at a temperature of 1550–1600 °C. About 20 g of As_2O_3 was added into the sample to help complete degassing of the melts, which results in *ca.* 3500 µg g^{-1} As in final glasses. A thin-walled platinum crucible was used to contain the melts. The melts were held at 1550 to 1600 °C for 4 h and then stirred for 5 h at a

speed of 20 rpm using a Pt80Rh20 spindle immersed into the melts. Stirring is a necessary procedure to achieve complete homogeneity of the highly viscous melt (Jochum *et al.* 2000). The spindle was removed from the melt, and the melt removed rapidly from the furnace and quenched by pouring into a custom designed mould at ambient temperature. Homogeneous, bubble-free glass blocks of about 3.0 kg were obtained by this procedure. The glasses were further annealed at 600 °C for 1 h and then cut as 10 mm × 10 mm × 3 mm glass splits ($n > 800$).

Because of long and high-temperature melting procedure, loss of volatile (e.g., Tl) was unavoidable. Potential sources of contaminations included Pt crucibles, remnants of previous samples and all other furnace components. ARM-2 glass was contaminated by the remnants of previous samples (Li, B, Zn and Yb) that were fused previously in the same crucible. However, even though the melts might be depleted by volatility or contaminated by furnace components, stirring and homogenisation ensured homogeneity of elements.

Analytical techniques for ARM glasses

The ARM glasses were characterised by different bulk and microanalytical techniques in ten laboratories from five institutions: MPI Mainz (Germany), NRCG, Beijing, China, Institute of Geology and Geophysics, Chinese Academy of Sciences, China (IGGCAS), Leibniz Universiät Hannover, Germany (LUH) and China University of Geosciences, Beijing, China (CUG). Electron probe microanalysis (EPMA) was conducted at LUH for major element characterisation.

Two ICP-OES analyses were undertaken at NRCG and IGGCAS, respectively. The digestion procedure is given by Wu *et al.* (2014). X-ray fluorescence spectrometry (XRF) was performed at IGGCAS. Two ICP-MS analyses were conducted for trace element characterisation at NRCG and IGGCAS, respectively. Two LA-Q-ICP-MS measurements were performed at CUG and IGGCAS. Two LA-SF-ICP-MS measurements were conducted at MPI Mainz and IGGCAS, respectively. The analytical procedure at MPI Mainz is given by Jochum *et al.* (2007). The analytical procedure at IGGCAS is similar as outlined by Wu *et al.* (2018b). All the LA-ICP-MS measurements used NIST SRM 610 as the calibration material and Ca as the internal standard. The Ca values were collected as averaged results from XRF, ICP-OES and EPMA. The detail information on the above analytical techniques is summarised in Appendix S2.

Acquisition method for LA-SF-ICP-MS

Seventy-seven isotopes (from ^{7}Li to ^{238}U for sixty-eight elements) could be swept in only 1 s using this acquisition method. The dwell time and mass settling times (both for electrostatic analyser jumps and for magnet jumps, including the jump back from ^{238}U to ^{7}Li) are given in Appendix S1 (Table S2). This method covers almost all elements of interest in geochemistry (e.g., LILE, HFSE, REEs and Th, U). The total sampling time for all scanned isotopes was 770 ms and total magnet settling time was 230 ms. Hence, the acquisition efficiency is estimated at about 77%. This acquisition method was achieved by simply reducing the magnet settling time and the number of samplings per peak (see details in Appendix S1, Table S2). For this approach, the

Mix oxide powders in proportion with the major element composition of andesite
Dope with 54 trace elements using oxide powders; Th and U using element solution
Homogenise in a ball mill

Transfer to a platinum crucible and pre-heat to 1000 °C

Melt at 1550–1600 °C for over 4 hours

Stir at a speed of 20 rpm at 1550–1600 °C for over 5 hours

Pour into customised mould to form a rectangular glass plate

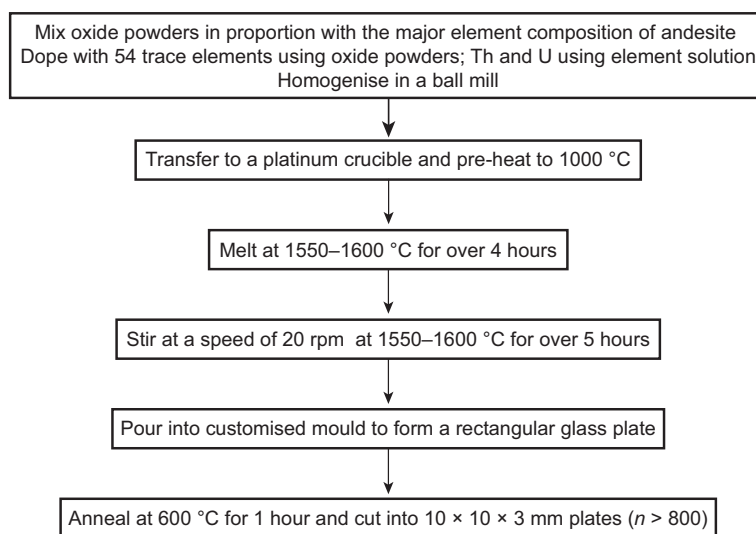Anneal at 600 °C for 1 hour and cut into 10 × 10 × 3 mm plates ($n > 800$)

Figure 1. Scheme of the preparation of ARM glasses.

stability, as revealed by the intermediate measurement precision, and the accuracy, as demonstrated by measurement data of reference glasses, needed to be confirmed for practical application of this acquisition method (as outlined in the Results and discussion section).

The experiments were performed at Geowissenschaftliches Zentrum Göttingen, University of Göttingen Germany (GZG) and IGGCAS. A RESOlution M-50 laser ablation system (Australian Scientific Instruments, Australia) coupled to an Element 2 sector-field ICP-MS (Thermo Fisher Scientific, Bremen, Germany) was used in GZG. A Photo Machine G2 laser ablation system (Teledyne CETAC technologies, USA) coupled to an Element XR sector-field ICP-MS (Thermo Fisher Scientific, Bremen, Germany) was used in IGGCAS. Daily optimisation of instrumental performance with NIST SRM 612 involved maximising the signal-to-background intensity ratios for Sr, La and U, while satisfying low oxide production rates ($ThO^+/Th^+ < 0.5\%$), low secondary ions ($Ca^{2+}/Ca^+ < 1.0\%$) and robust plasma conditions (sensitivity ratio S (U^+)/S (Th^+) in a range of 0.95–1.05).

Homogeneity test

The homogeneity of the glass at bulk and microscale was evaluated using ICP-OES, ICP-MS, EPMA, LA-Q-ICP-MS and LA-SF-ICP-MS. For the bulk-scale homogeneity test, ICP-OES and ICP-MS techniques were used. Both techniques require 50–100 mg samples. The homogeneity of major elements was evaluated using EPMA technique at LUH. For this approach, the homogeneity was assessed by comparing the standard deviation of all measurements ($n = 30$) with the predicted error resulting from the counting statistics of the raw signals. The error by counting statistics took the Gaussian error propagation of the respective three measurement signals (peak signal, lower-, upper-background signal) into account. Three laboratories (MPI, IGGCAS and CUG) conducted a LA-Q (SF)-ICP-MS homogeneity test. For this technique, we define chemical heterogeneities as variations in elemental mass fraction that are excess of the analytical precision.

Results and discussion

Capability of LA-SF-ICP-MS for large mass range (^{7}Li to ^{238}U) multiple-element determination

Analytical results of the andesitic MPI-DING StHs6/80-G ($n = 359$), which were collected at GZG over 3 years from 2015 to 2017, are provided to demonstrate the precision and accuracy of the proposed method. The (long-term) analytical reproducibility is plotted in Figure 2. Analytical results were calculated using NIST SRM 610 as calibration material and Ca as an internal standard. Figure 2a documents the long-term analytical reproducibility (given as 1RSD %) of Ce in StHs6/80-G is 3.94%, which is around two times larger than the short-term precision (Appendix S3, Figure S1). For practical purposes, it is reasonable to take the daily instrumental variation into consideration rather than long-term variations over years. Figure 2b shows the histogram distribution of Ce results ($n = 359$) that clearly
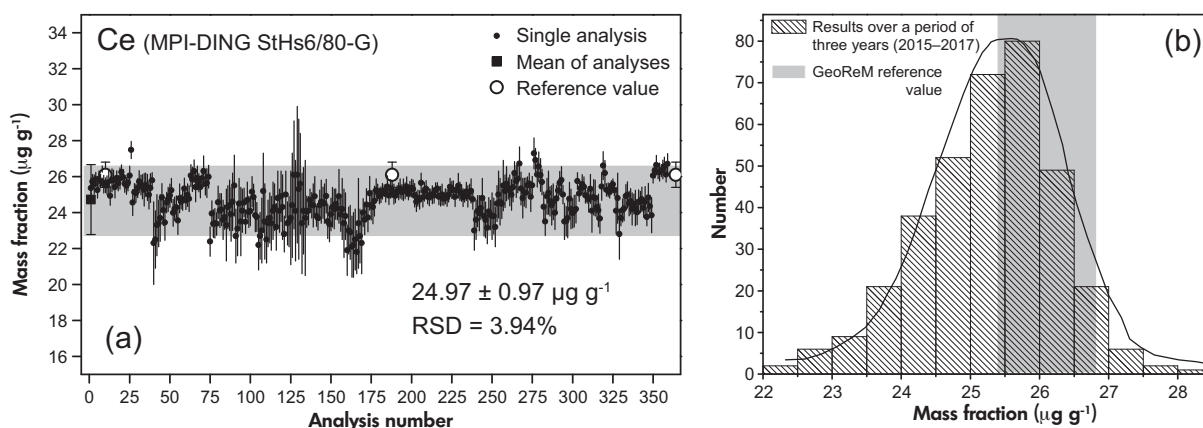
Figure 2. (a) The variability of Ce mass fraction in StHs 6/80-G from 359 analyses over 3 years (2015–2017). The grey zone represents two times the standard deviation based on 359 individual measurements. (b) Frequency distribution of Ce mass fractions in StHs6/80-G. 'mean ± 1s' were calculated based on 359 analyses. The Ce mass fraction in StHs6/80-G was calibrated using NIST SRM 610 as the measurement standard and Ca as the internal standard element.
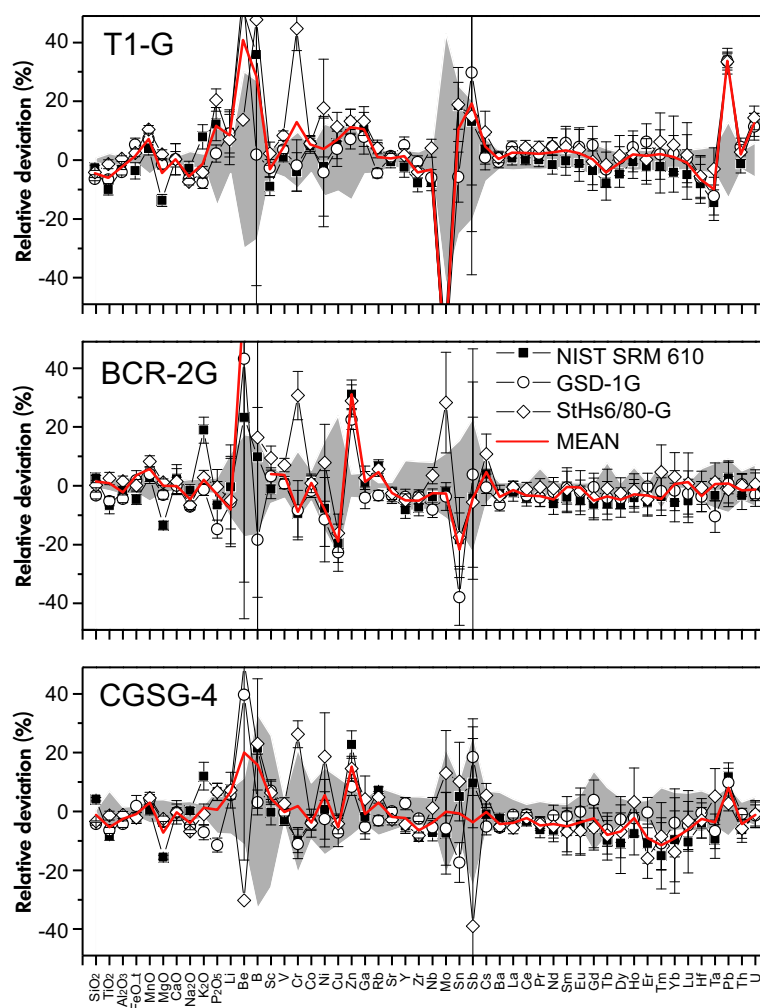
Figure 3. Plots of relative deviations for fifty elements mass fractions of T1-G, BCR-2G and CGSG-4. Data were calculated using NIST SRM 610, GSD-1G and StHs6/80-G as calibration materials, and Ca as internal standard element. The red line represents the mean results from using three calibrators. The relative deviations are given as the discrepancy (%) with the reference values [(analysed results-reference values)/reference values *100]. The results and standard deviations of T1-G, BCR-2G and CGSG-4 are derived from 78, 73 and 29 repeated analyses. The grey zone represents the uncertainty of reference values at 95% confidence level. The results of our major element analysis match reference values within 5%, except TiO$_2$, FeO, MgO, K$_2$O that were calibrated using NIST SRM 610. Trace elements results are in agreement with reference values within 10%. Exceptions are observed for Pb in T1-G and Zn in BCR-2G and CGSG-4. [Colour figure can be viewed at wileyonlinelibrary.com]

indicates a Gaussian distribution, further demonstrating that the stability of our acquisition method is practical for multiple-element quantification.

To validate the accuracy of this acquisition method, T1-G, BCR-2G and CGSG-4 reference glasses were analysed using NIST SRM 610, StHs 6/80-G and GSD-1G as calibration materials and Ca as internal standard (Figure 3). Reference values of these calibration materials are summarised in Appendix S1 (Table S3). The results of our major element analysis match reference values within ± 5%,

except TiO$_2$, FeO, MgO, K$_2$O that were calibrated using NIST SRM 610. Trace elements results are in agreement with reference values within ± 10%. Data consistency is also confirmed by evaluating the smoothness REE chondrite-normalised patterns (see Appendix S3, Figure S2). Exceptions are observed for Pb in T1-G and Zn in BCR-2G and CGSG-4. We also found mass fractions of Cr in T1-G, BCR-2G and CGSG-2 that are calibrated using StHs6/80-G to be consistently higher than that of using NIST SRM 610 and GSD-1G. These biases are mainly attributed to the calibration procedure, potential inhomogeneity and/or the larger

Table 1.
LA-SF-ICP-MS measurement results for USGS NKT-1G and TB-1G reference glasses

Elements	USGS NKT-1G			USGS TB-1G		
	Information value	This study (n = 8)		Information value	This study (n = 8)	
		Value	2s		Value	2s
SiO_2	38.9	38.6	1.9	54.3	53.8	1.1
TiO_2	3.92	3.64	0.09	0.84	0.87	0.04
Al_2O_3	10.5	10.1	0.5	17.1	16.5	0.6
FeO(t)	12.2	12.4	0.5	8.67	8.27	0.54
MnO	0.24	0.21	0.03	0.18	0.18	0.02
MgO	14.2	14.0	1.8	3.51	3.51	0.07
CaO	13.4	–	–	6.7	–	–
Na_2O	3.85	3.48	0.19	3.56	3.10	0.09
K_2O	1.27	1.33	0.14	4.52	4.43	0.31
P_2O_5	0.95	0.95	0.15	0.61	0.56	0.07
Li	–	–	–	–	–	–
Be	–	–	–	–	–	–
B	–	–	–	–	–	–
Sc	–	23.3	2.3	23.0	22.6	3.0
V	–	300	10	179	199	7
Cr	–	508	184	55.8	56.1	3.0
Co	–	67.2	2.3	22.8	23.2	1.1
Ni	–	352	41	14.5	17.6	0.4
Cu	–	54.3	4.4	76.1	79.4	6.7
Zn	–	152	25	106	127	21
Ga	–	27.7	1.1	23.6	23.2	1.4
Rb	30.7	33.7	3.1	142	151	10
Sr	1195	1192	30	1352	1295	41
Y	32.0	27.6	2.1	26.4	23.4	2.6
Zr	310	278	30	245	224	32
Nb	95.9	89.9	6.8	29.8	27.7	2.2
Mo	–	0.86	0.14	–	1.45	0.15
Sn	–	2.95	0.58	–	1.76	0.19
Sb	–	–	–	–	–	–
Cs	0.53	0.55	0.10	–	2.71	0.43
Ba	753	773	58	976	939	50
La	63.3	63.5	2.0	44.1	43.5	1.6
Ce	126	134	5	92.0	87.4	1.8
Pr	15.0	15.1	0.7	10.7	9.9	0.4
Nd	61.4	61.3	1.9	40.1	38.2	2.4
Sm	12.3	12.0	0.4	7.23	6.99	0.49
Eu	3.75	3.73	0.18	1.81	1.73	0.12
Gd	10.1	10.1	0.7	5.79	5.65	0.61
Tb	1.30	1.27	0.07	0.78	0.76	0.06
Dy	6.69	6.64	0.68	4.79	4.38	0.61
Ho	1.09	1.08	0.06	0.90	0.86	0.08
Er	2.54	2.53	0.29	2.67	2.53	0.38
Tm	0.30	0.30	0.03	0.41	0.36	0.04
Yb	1.79	1.72	0.18	2.64	2.47	0.30
Lu	0.23	0.22	0.02	0.39	0.37	0.05
Hf	6.44	6.34	0.39	5.93	5.46	0.34
Ta	4.99	4.70	0.58	1.60	1.40	0.17
Pb	3.10	3.59	0.87	16.8	18.1	4.4
Th	7.35	6.87	0.44	15.1	13.8	1.2
U	2.28	2.23	0.17	4.11	4.08	0.24

Element mass fractions were calculated as the mean using NIST SRM 610, MPI-DING StHs6/80-G and USGS GSD-1G as calibration materials with Ca as the internal standard element. Major and trace element mass fractions are given in % m/m and µg g^{-1}, respectively. '–' means that data are not available or lower than the detection limit. 2s is derived from the corresponding number of measurements. Several elements due to low mass fractions (Ti, Fe, Mn, Mg, K and P in NIST SRM 610, Be, Mo and Sb in StHs6/80-G) or potential under/overestimated certified values (Cr, Ni in StHs6/80-G and Sn, Sb in GSD-1G) may result in imprecise calibrations. Thus, these elements in corresponding calibration materials were not used for the calibration procedure.

Table 2.
Major element mass fractions in ARM-1, ARM-2 and ARM-3

	ICP-OES [a] (n = 4)		ICP-OES [b] (n = 4)		XRF (n = 3)		EPMA (n = 30)		LA-ICP-MS (n = 225)	
	Value	2s	Value	2s	Value	2s	Value	2s	Value	2s
ARM-1										
SiO_2	–	–	58.4	0.1	58.1	0.4	58.7	0.4	–	–
TiO_2	0.94	0.01	1.02	0.02	0.99	0.01	0.99	0.06	0.95	0.07
Al_2O_3	13.2	0.2	13.3	0.1	13.4	0.1	13.4	0.4	–	–
FeO(t)	5.67	0.03	5.79	0.02	5.61	0.02	5.79	0.26	–	–
MnO	0.05	0.01	0.05	0.02	0.02	0.01	0.04	0.04	0.05	0.01
MgO	3.64	0.03	3.95	0.01	3.75	0.02	3.76	0.12	–	–
CaO	5.00	0.05	5.09	0.06	5.08	0.02	5.12	0.22	–	–
Na_2O	4.47	0.07	4.44	0.03	4.43	0.02	4.36	0.20	–	–
K_2O	3.11	0.03	3.16	0.03	3.13	0.02	3.12	0.08	–	–
P_2O_5	–	–	0.25	0.03	0.27	0.01	0.26	0.06	0.27	0.05
SUM			95.5		94.8		95.5			
ARM-2										
SiO_2	–	–	58.3	0.1	57.6	0.3	57.8	0.5	–	–
TiO_2	0.92	0.01	1.03	0.02	0.97	0.01	0.97	0.06	0.99	0.09
Al_2O_3	13.0	0.2	13.3	0.1	13.0	0.1	13.1	0.2	–	–
FeO(t)	5.63	0.14	5.84	0.07	5.68	0.04	5.71	0.24	–	–
MnO	0.05	0.01	0.05	0.05	0.05	0.01	0.06	0.06	0.06	0.01
MgO	3.65	0.07	3.90	0.01	3.76	0.02	3.65	0.20	–	–
CaO	4.89	0.11	5.04	0.02	5.06	0.04	5.05	0.24	–	–
Na_2O	4.36	0.09	4.44	0.04	4.48	0.01	4.40	0.22	–	–
K_2O	2.92	0.05	3.04	0.02	3.00	0.02	3.05	0.10	–	–
P_2O_5	–	–	0.30	0.02	0.28	0.01	0.30	0.14	0.28	0.06
			95.2		93.8		94.1			
ARM-3										
SiO_2	–	–	60.8	0.1	60.3	0.5	60.4	0.6	–	–
TiO_2	0.97	0.01	1.06	0.02	1.01	0.01	1.02	0.06	1.01	0.10
Al_2O_3	13.8	0.3	13.8	0.1	13.8	0.1	13.8	0.2	–	–
FeO(t)	5.95	0.10	5.77	0.09	5.92	0.02	6.00	0.24	–	–
MnO	0.05	0.01	0.05	0.02	0.05	0.01	0.05	0.04	0.05	0.01
MgO	3.41	0.04	3.63	0.01	3.52	0.01	3.50	0.16	–	–
CaO	5.25	0.07	5.34	0.09	5.37	0.05	5.34	0.30	–	–
Na_2O	4.64	0.06	4.62	0.06	4.64	0.02	4.74	0.24	–	–
K_2O	3.14	0.06	3.25	0.11	3.16	0.05	3.18	0.08	–	–
P_2O_5	–	–	0.26	0.03	0.28	0.01	0.31	0.16	0.28	0.06
			98.56		97.99		98.35			

ARM-1, ARM-2 and ARM-3 were analysed by XRF, ICP-OES and EPMA. Data are given in % *m/m*. ICP-OES [a] represents ICP-OES at IGGCAS. ICP-OES [b] represents ICP-OES at NRCG.

uncertainty of reference values. It is important to point out that, although we collected signal data for sixty-eight elements, only fifty elements were quantified, mainly because of very low mass fractions that are near or below the detection limit for the other elements. In Appendix S3 (Figure S3), we compare the results of NIST SRM 612, ML3B-G and BCR-2G obtained from GZG and IGGCAS. These two independent laboratories yielded very similar and accurate results, further demonstrating the reliability of our LA-SF-ICP-MS technique for multiple-element quantification.

All the above results indicate that our acquisition method for Element 2 or Element XR is useful for a wide mass range (from ^7Li to ^{238}U) multiple-element quantification and yields reliable results. Compared with Q-ICP-MS, the sensitivity of

Element 2 or Element XR is higher by a factor of 3–5, which allows smaller beam sizes and thus results in improved spatial resolution. Here, the results of USGS NKT-1G and TB-1G using the LA-SF-ICP-MS are reported (Table 1). Information values collected from Elburg *et al.* (2005) and Kimura and Chang (2012) are listed for comparison (Table 1). The values of these two reference glasses have been rarely reported, and our data may be useful for the certification procedures.

Homogeneity

The homogeneity of major and trace elements is a fundamental requirement of any reference material. Tables 2 and 3 illustrate that there is no statistical difference between
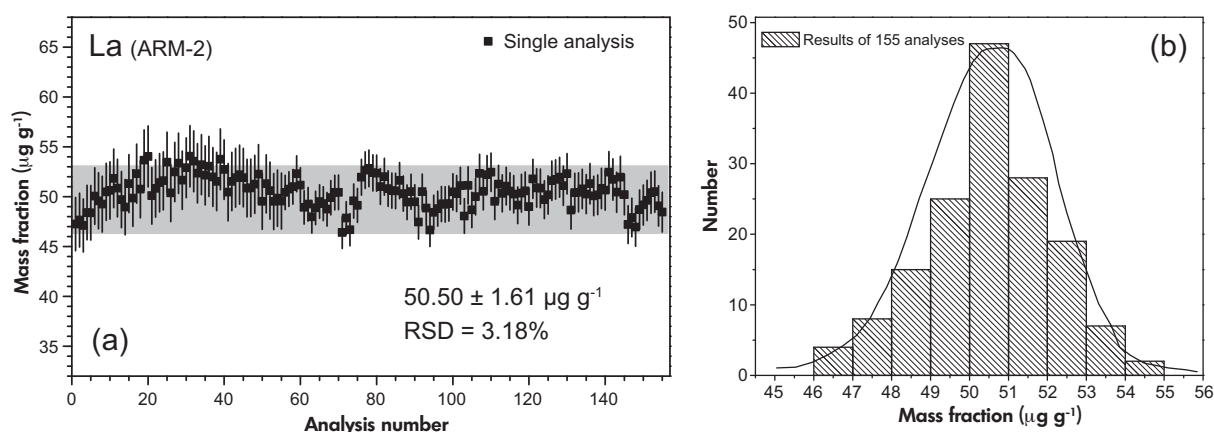
Figure 4. (a) The variability of La mass fraction in ARM-2 with 155 spot analyses in thirty-one individual glass splits. Five spot analyses for each glass split. The grey zone represents two times the standard deviation based on 155 measurements. (b) Frequency distribution of La mass fractions in ARM-2. 'mean ± 1s' were calculated based on 155 analyses. The La mass fraction in ARM-2 was calculated using NIST SRM 610 for calibration and Ca as internal standard element. The laser spot size was 50 μm.
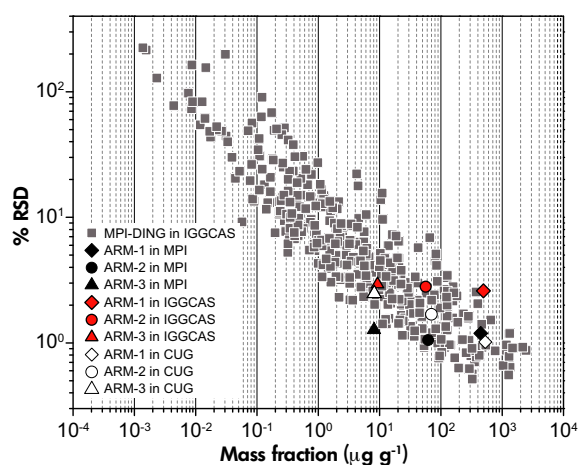
Figure 5. Comparison of RSD between the well-characterised MPI-DING and ARM glasses. Trace elements include Sc, Rb, Sr, Y, Zr, Nb, Cs, Ba, La, Ce, Pr, Nd, Sm, Eu, Gd, Tb, Dy, Ho, Er, Tm, Yb, Lu, Ta, Th, U, V, Cr, Co, Ni, Cu, Zn, Ga, Mo, Sn, Sb, W, Tl, Pb and Bi. The results were calibrated using NIST SRM 610 as calibration material and Ca as internal standard element. Plots of ARM glass are the mean of the trace elements mentioned above. Mass fractions in μg g^{-1}. [Colour figure can be viewed at wileyonlinelibrary.com]

two ICP-OES and two ICP-MS measurements, except for TiO$_2$ and MgO, which are presumably caused by a systematic analytical bias of the technique using different calibration procedures. The obtained homogeneity factors (standard deviation/predicted error) from EPMA for major elements scatter around unity and do not exceed a value of

2.0 (Harries 2014). Therefore, all these ARM glasses can be regarded as homogeneous within the spatial resolution (10 μm) of the microprobe for all major elements.

The homogeneity within and between glass splits of trace elements was evaluated using the LA-Q (SF)-ICP-MS in three laboratories. In IGGCAS, thirty-one glass splits were randomly picked from ~ 800 splits for each ARM glass. Five spot analyses (spot size: 50 μm) have been randomly located in each glass split. Figure 4 plots the La mass fractions obtained for ARM-2. A total of 155 spot analyses yielded an RSD of 3.18%, which is comparable to that of well-characterised and homogenous MPI-DING reference glasses (Figure 5). The data scatter follows a Gaussian distribution. Appendix S3 (Figure S4) shows the RSDs of other elements in ARM glasses. Most RSDs are smaller than 4%, except Be and Cr in ARM-1 glasses. LA-SF-ICP-MS measurements at MPI were done on five glass splits randomly picked from a total of ~800 splits. Each glass was analysed with nine spots (spot size: 80 μm) and nine lines (spot size: 80 μm, length: 300 μm). Spot analysis yields an RSD of only about 1.2%, which emphasises the high homogeneity of the glasses and the reproducibility of the measurements as well. The mean RSD for the line scanning analysis is about 2% except for ARM-3 (ca. 7%), which is caused by one extremely high outlier value. We attribute these high outlier values to instrument/technical problems instead of random scatters. At CUG, homogeneity was evaluated on a large glass split (10 mm × 10 mm) with a profile line analysis with 40 spots (spot size: 50 μm) at a spacing of approximately 150 μm. Mean RSD values were 1.0%, 1.7% and 2.5% for ARM-1, ARM-2 and ARM-3, respectively.
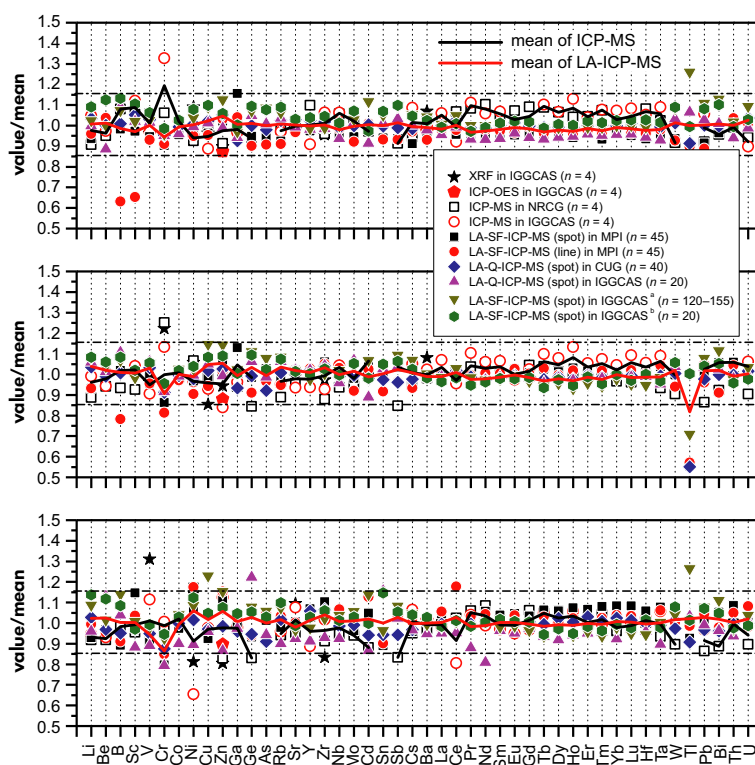
Figure 6. Comparison of trace element results of ARM-1, ARM-2 and ARM-3 from XRF, ICP-OES, ICP-MS, LA-Q-ICP-MS and LA-SF-ICP-MS. The y-axes (values/mean) represent the ratios of results from individual techniques to the mean of all techniques. [Colour figure can be viewed at wileyonlinelibrary.com]

In Figure 5, a comparison of the RSD between well-characterised MPI-DING glasses and ARM glasses is plotted. There is a significant negative linear correlation between mass fraction and RSD on a logarithmic scale for MPI-DING glasses. This trend follows a Poisson counting uncertainty, demonstrating that the measurement reproducibility is derived from the counting statistics of the measurements. Therefore, the RSD obtained for MPI-DING glass defines the LA-ICP-MS analytical precision. The results illustrate that the mean of RSD of ARM-1, ARM-2 and ARM-3 from all three laboratories is within the range of the LA-ICP-MS measurement precision. This demonstrates that the homogeneity of our new ARM glasses is as good as the well-characterised MPI-DING glasses, which are widely used as LA-ICP-MS reference materials (Jochum *et al.* 2000, 2006). Homogeneity of the three ARM glasses was further demonstrated by ICP-OES, ICP-MS, EPMA and LA-ICP-MS measurements on a small scale (within a glass split) and large scale (between glass splits) (see Tables 2 and 3).

Characterisation of the ARM glasses

Table 2 lists the measurement results for major elements in the ARM glasses obtained by XRF, ICP-OES, EPMA and

LA-ICP-MS (only for TiO_2, MnO and P_2O_5) and includes the total analytical uncertainties (%) of the used techniques. The consistency of the mass fraction data obtained by different methods is a measure of their analytical quality. Two ICP-OES analyses of ARM glasses were performed on different glass splits. The data agree within 3% of relative deviation, except TiO_2 and MgO. These differences are presumably caused by a systematic analytical bias of the technique using different calibration procedures, because these differences were observed for all ARM glasses. The total major oxides are below 100%, which is due to the addition of about 0.5% As_2O_5 to assure degassing of the melts, contamination by the Li-B flux (only for ARM-2) and of trace elements added (in particular for ARM-1).

Table 3 summarises the trace element data for the ARM glasses obtained by XRF, ICP-OES, ICP-MS and LA-ICP-MS. Two ICP-MS analyses were performed on different glass splits. All LA-ICP-MS data were calibrated with NIST SRM 610 and using Ca as the internal standard. Calcium contents were taken as the mean of XRF, ICP-OES and EPMA measurements. This may be important for data traceability and comparison with other data from other techniques. Figure 6 illustrates that all data agree well for most elements,

Table 3.
Measurement results for trace elements in ARM-1, ARM-2 and ARM-3 determined by XRF, ICP-OES, ICP-MS and LA-ICP-MS

| | XRF | | ICP-OES[2] | | ICP-MS[1] | | ICP-MS[2] | | LA-SF-ICP-MS[3] Spot | | LA-SF-ICP-MS[3] Line | | LA-Q-ICP-MS[4] Spot | | LA-Q-ICP-MS[1] Spot | | LA-SF-ICP-MS[1] Spot (Exp.1) | | LA-SF-ICP-MS[1] Spot (Exp.2) | |
| | n = 4 | | n = 4 | | n = 4 | | n = 4 | | n = 45 | | n = 45 | | n = 40 | | n = 20 | | n = 100 | | n = 15 | |
	Values	2s	Values	2s	Values	2s	Values	2s	Values	2s	Values	2s	Values	2s	Values	2s	Values	2s	Values	2s
ARM-1																				
Li	—	—	—	—	464	4	535	35	478	3	490	21	528	8	510	17	523	25	557	16
Be	—	—	—	—	452	9	463	23	486	11	492	13	475	19	420	22	475	18	534	15
B	—	—	—	—	500	5	—	—	455	9	292	19	467	20	504	23	497	28	524	7
Sc	—	—	—	—	453	9	481	27	417	7	280	16	451	7	438	7	438	18	474	7
V	553	8	—	—	608	8	557	37	544	14	535	28	592	11	584	6	591	19	611	5
Cr	438	6	—	—	492	9	614	31	418	6	422	19	442	8	440	16	444	17	456	11
Co	—	—	—	—	506	6	508	31	475	6	503	15	494	8	477	6	505	11	510	5
Ni	515	11	—	—	438	7	451	29	454	6	448	22	476	9	470	13	491	14	510	8
Cu	430	40	—	—	450	8	396	30	430	5	426	18	457	8	452	5	487	14	491	2
Zn	501	12	488	4	510	13	580	27	571	35	575	34	588	13	552	24	629	44	591	7
Ga	—	—	—	—	488	9	472	25	565	11	509	16	453	22	461	10	475	18	491	6
Ge	—	—	—	—	588	9	—	—	593	8	564	19	626	7	655	19	670	27	685	6
As	—	—	—	—	—	—	—	—	3160	180	3050	180	3290	70	3380	60	3650	150	3620	50
Rb	—	—	—	—	477	13	471	31	449	8	443	16	498	9	503	13	517	12	530	5
Sr	458	4	—	—	469	8	458	28	453	5	450	9	479	8	461	3	477	19	480	8
Y	—	—	—	—	493	10	409	28	437	13	444	31	460	8	441	1	443	26	467	8
Zr	417	1	—	—	419	9	465	26	430	13	438	28	445	7	430	5	432	25	456	11
Nb	—	—	—	—	498	8	501	31	452	3	463	6	466	7	442	3	471	16	477	5
Mo	—	—	—	—	496	3	—	—	459	1	447	18	485	10	492	6	500	18	520	4
Cd	—	—	—	—	450	6	—	—	467	16	468	28	465	15	423	21	517	33	451	10
Sn	—	—	—	—	—	—	—	—	556	8	552	17	590	1	598	10	622	26	633	5
Sb	—	—	—	—	487	8	—	—	500	21	497	18	528	10	550	10	585	22	586	6
Cs	—	—	—	—	448	6	515	33	433	10	460	25	467	7	475	4	499	23	496	34
Ba	2170	40	1970	20	2070	30	2020	120	19200	40	18900	80	2060	34	1990	20	2120	80	2080	20
La	—	—	—	—	471	5	480	31	436	11	443	19	452	8	432	5	456	23	449	4
Ce	—	—	—	—	475	5	409	33	425	9	435	17.3	456	7	446	5	466	18	449	6
Pr	—	—	—	—	467	5	478	29	407	7	415	13	425	7	402	5	431	21	419	4
Nd	—	—	—	—	486	4	466	28	417	7	431	15	435	8	411	5	441	23	436	10
Sm	—	—	—	—	483	7	494	32	442	9	450	18	463	9	433	7	465	28	468	10
Eu	—	—	—	—	490	9	452	27	436	6	441	13	463	7	440	3	468	27	467	7
Gd	—	—	—	—	487	6	445	25	427	12	442	24	445	8	419	10	446	30	454	8
Tb	—	—	—	—	474	5	480	27	411	9	419	21	431	6	406	4	431	31	430	7

Table 3 (continued).
Measurement results for trace elements in ARM-1, ARM-2 and ARM-3 determined by XRF, ICP-OES, ICP-MS and LA-ICP-MS

	XRF		ICP-OES [2]		ICP-MS [1]		ICP-MS [2]		LA-SF-ICP-MS [3]				LA-Q-ICP-MS [4]		LA-Q-ICP-MS [1]		LA-SF-ICP-MS [1]			
									Spot		Line		Spot		Spot		Spot (Exp.1)		Spot (Exp.2)	
	n = 4		n = 4		n = 4		n = 4		n = 45		n = 45		n = 40		n = 20		n = 100		n = 15	
	Values	2s	Values	2s	Values	2s	Values	2s	Values	2s	Values	2s	Values	2s	Values	2s	Values	2s	Values	2s
Dy	—	—	—	—	482	6	482	31	434	12	443	27	449	7	426	5	449	31	456	8
Ho	—	—	—	—	468	7	508	29	423	11	429	29	446	7	426	4	446	31	451	10
Er	—	—	—	—	482	7	480	28	446	15	450	28	461	7	442	3	458	36	471	6
Tm	—	—	—	—	454	6	455	28	395	11	404	27	423	7	403	5	420	31	429	9
Yb	—	—	—	—	453	6	494	29	443	15	460	24	459	8	440	11	460	35	472	10
Lu	—	—	—	—	449	5	483	30	424	15	429	26	451	7	428	3	446	35	458	8
Hf	—	—	—	—	495	6	481	32	428	18	440	31	459	8	431	5	454	34	470	12
Ta	—	—	—	—	465	2	495	28	435	13	445	12	452	8	422	2	459	33	462	7
W	—	—	—	—	416	3	—	—	426	9	421	17	460	8	469	5	493	21	495	4
Tl	—	—	—	—	—	—	—	—	30.4	0.6	31.4	1.3	32.0	0.94	37.3	0.83	44.2	1.78	34.9	0.61
Pb	—	—	—	—	566	7	649	36	561	12	545	23	615	11	631	6	681	30	664	8
Bi	—	—	—	—	566	11	—	—	570	16	497	16	589	11	597	10	668	36	652	5
Th	—	—	—	—	12.3	0.2	—	—	12.6	0.3	12.9	0.6	12.5	0.3	11.7	0.32	12.7	1.05	12.4	0.16
U	—	—	—	—	11.8	0.10	11.2	1.03	12.5	0.2	12.6	0.5	12.9	0.35	12.3	0.27	13.6	0.63	12.8	0.40
ARM-2																				
Li	—	—	—	—	1100	30	1220	20	11500	10	11500	20	1280	30	1310	30	1340	40	1340	10
Be	—	—	—	—	51.5	2.0	51.6	1.3	55.4	1.0	54.8	1.2	54.2	3.8	55.4	7.4	56.8	3.8	58.0	6.4
B	—	—	—	—	9810	460	—	—	10700	400	8220	220	10560	360	11610	290	112200	530	11370	140
Sc	53.7	5.3	—	—	47.7	1.1	53.6	1.0	51.7	0.7	52.5	1.4	51.7	1.1	51.7	0.7	50.7	2.6	52.6	1.4
V	74.6	2.4	—	—	54.8	0.9	50.6	1.0	55.5	0.7	53.4	0.6	57.7	1.4	59.3	1.6	58.8	2.1	58.9	1.1
Cr	—	—	—	—	76.4	2.5	69.1	2.0	52.7	1.3	49.7	1.0	55.7	1.5	55.8	2.8	57.0	3.1	58.3	7.1
Co	62.6	5.2	—	—	58.6	1.1	60.0	1.2	60.0	0.9	57.8	1.2	59.2	1.5	59.0	2.0	61.1	1.9	60.6	0.6
Ni	—	—	—	—	63.1	0.8	57.2	1.5	57.3	1.9	53.5	2.7	57.9	2.5	58.9	3.2	60.7	2.6	61.5	1.3
Cu	47.5	6.1	—	—	55.0	2.9	51.7	1.7	54.8	1.2	52.5	1.0	56.6	1.5	58.3	0.6	63.8	2.6	60.3	0.8
Zn	4830	70	4500	70	5130	70	4290	90	5480	110	5190	190	5260	120	5080	1700	5850	300	5580	100
Ga	—	—	—	—	65.7	1.1	67.3	0.5	79.0	2.5	70.3	1.1	65.3	2.0	69.9	2.3	71.4	4.5	70.2	1.1
Ge	—	—	—	—	57.7	1.5	—	—	67.3	0.7	62.2	1.6	67.8	1.7	72.6	3.6	75.9	4.0	74.8	4.0
As	—	—	—	—	—	—	—	—	3570	100	3350	120	3200	70	3430	50	3750	170	3560	40
Rb	63.6	1.0	—	—	51.3	2.5	54.9	1.1	56.5	0.7	54.6	1.3	58.1	1.7	61.2	1.8	62.5	1.9	61.9	0.6
Sr	—	—	—	—	61.4	0.8	60.1	1.1	65.7	0.3	65.6	1.1	65.6	1.4	65.5	1.4	65.4	2.6	65.1	0.7
Y	55.3	1.8	—	—	51.1	1.0	47.8	1.3	51.9	0.9	52.5	1.9	52.0	1.3	52.0	2.1	49.8	2.8	51.2	1.3
Zr	—	—	—	—	50.0	0.9	52.7	1.3	60.2	1.2	59.7	2.1	59.1	1.6	59.2	1.7	57.0	3.4	58.3	1.8
Nb	—	—	—	—	54.1	1.2	60.2	1.5	59.2	1.0	59.5	1.0	57.1	1.3	55.3	0.6	58.9	2.0	57.5	0.8
Mo	—	—	—	—	54.1	1.4	—	—	56.1	1.1	52.6	1.3	56.9	2.1	61.1	1.5	59.6	2.7	60.3	1.9

Table 3 (continued).
Measurement results for trace elements in ARM-1, ARM-2 and ARM-3 determined by XRF, ICP-OES, ICP-MS and LA-ICP-MS

	XRF		ICP-OES [2]		ICP-MS [1]		ICP-MS [2]		LA-SF-ICP-MS [3]				LA-Q-ICP-MS [4]		LA-Q-ICP-MS [1]		LA-SF-ICP-MS [1]			
									Spot		Line		Spot		Spot		Spot (Exp.1)		Spot (Exp.2)	
	n = 4		n = 4		n = 4		n = 4		n = 45		n = 45		n = 40		n = 20		n = 100		n = 15	
	Values	2s	Values	2s	Values	2s	Values	2s	Values	2s	Values	2s	Values	2s	Values	2s	Values	2s	Values	2s
Cd	—	—	—	—	49.9	0.8	—	—	53.5	0.8	51.5	1.7	49.2	3.1	44.6	4.0	53.6	3.5	49.3	0.9
Sn	—	—	—	—	—	—	—	—	71.7	0.8	66.7	1.3	70.9	2.1	74.6	2.3	76.2	2.7	76.4	2.0
Sb	—	—	—	—	53.1	0.3	—	—	64.8	1.1	60.3	1.9	60.2	1.8	64.9	1.6	68.5	3.1	66.6	0.9
Cs	—	—	—	—	49.2	0.7	54.6	1.0	50.2	0.7	48.5	1.6	50.8	1.4	53.5	1.3	55.6	2.3	53.2	0.4
Ba	269	78	248	3	245	2	255	5	242	3	244	4	246	6	247	6	250	9	245	6
La	—	—	—	—	51.3	0.7	55.6	1.1	51.9	0.8	52.5	0.9	51.7	1.0	51.4	0.8	51.2	2.3	50.1	0.6
Ce	—	—	—	—	54.3	0.5	51.3	1.6	52.9	0.6	53.9	1.0	54.6	1.4	54.6	0.9	55.3	1.8	52.8	0.7
Pr	—	—	—	—	51.6	0.6	54.9	1.3	48.9	0.5	49.5	0.6	49.2	1.2	48.0	0.8	49.0	1.9	47.2	1.1
Nd	—	—	—	—	58.4	0.7	58.9	1.2	55.4	0.5	55.9	1.0	54.1	1.3	54.0	4.3	54.1	3.4	53.5	2.4
Sm	—	—	—	—	51.5	0.2	55.0	1.1	52.0	0.8	51.8	1.1	50.6	1.5	50.7	2.3	50.4	2.9	50.5	1.6
Eu	—	—	—	—	51.7	0.4	49.4	1.1	52.0	0.5	52.0	0.4	50.5	1.4	50.0	1.2	50.5	2.2	49.6	1.3
Gd	—	—	—	—	51.1	0.2	50.0	1.1	49.2	0.8	49.0	1.7	48.3	1.6	48.0	1.9	47.2	2.8	48.1	1.0
Tb	—	—	—	—	50.8	0.3	53.8	0.7	50.2	1.2	50.4	1.8	47.8	1.0	46.8	0.7	46.2	2.6	45.8	0.9
Dy	—	—	—	—	54.3	0.52	57.8	2.23	54.2	1.0	53.4	2.3	52.9	1.43	52.5	0.78	51.2	2.97	52.2	1.55
Ho	—	—	—	—	50.2	0.6	57.3	1.8	52.2	1.1	51.5	2.2	49.4	1.2	49.1	0.9	47.1	2.6	47.9	1.3
Er	—	—	—	—	52.8	0.5	55.7	1.1	53.7	1.2	52.6	2.6	52.7	1.4	52.4	2.2	50.5	3.0	52.2	1.3
Tm	—	—	—	—	50.5	0.6	53.2	1.6	51.0	1.3	50.4	2.4	48.8	1.3	48.5	0.8	46.7	2.7	47.2	0.8
Yb	—	—	—	—	646	8	699	25	668	18	674	21	671	16	670	8	653	38	668	18
Lu	—	—	—	—	46.7	0.6	53.1	1.9	49.7	1.3	49.6	2.2	48.3	1.2	47.9	0.9	46.3	2.7	47.2	0.9
Hf	—	—	—	—	51.5	0.6	54.4	1.3	52.4	1.5	51.7	2.5	51.0	1.4	50.9	1.7	48.8	3.1	51.5	1.3
Ta	—	—	—	—	47.8	1.1	55.8	1.7	53.0	1.0	53.4	1.0	50.7	1.4	48.7	0.8	50.5	2.6	49.5	0.6
W	—	—	—	—	50.6	1.0	—	—	55.8	0.6	52.6	0.5	56.2	2.0	57.9	2.1	59.3	2.2	59.1	1.2
Tl	—	—	—	—	—	—	0.30	0.20	0.10	0.01	0.10	0.01	0.10	0.02	0.20	0.09	0.10	0.03	0.10	0.02
Pb	—	—	—	—	65.9	0.9	79.4	2.6	76.7	1.6	73.1	2.2	74.4	2.2	78.8	1.1	82.2	3.2	79.2	0.5
Bi	—	—	—	—	64.6	0.5	64.4	1.2	73.9	0.4	63.7	1.8	69.8	2.3	71.6	1.0	78.0	3.5	73.6	0.8
Th	—	—	—	—	12.9	0.2	—	—	13.8	0.3	13.6	0.5	13.0	0.5	12.8	0.6	12.7	0.7	12.5	0.3
U	—	—	—	—	12.1	0.1	14.2	0.4	13.6	0.1	13.3	0.2	13.6	0.4	13.3	0.4	13.8	0.7	13.1	0.2
ARM-3																				
Li	—	—	—	—	17.1	0.3	17.6	0.7	17.3	0.4	18.5	3.9	19.2	1.2	17.9	3.0	20.3	1.3	21.2	1.4
Be	—	—	—	—	5.77	0.32	5.85	0.08	6.09	0.24	5.99	0.23	6.10	1.28	7.10	1.43	6.39	0.77	7.03	0.44
B	—	—	—	—	59.6	1.0	—	—	54.1	2.3	55.2	6.4	57.6	4.3	63.0	12.3	69.2	4.1	65.8	2.0
Sc	—	—	—	—	6.71	0.20	7.23	0.15	8.05	0.18	7.27	0.07	6.81	0.35	6.20	0.50	7.09	0.38	6.81	0.13
V	15.9	14.6	—	—	11.1	0.3	13.6	2.0	11.0	0.1	11.6	2.6	11.5	0.5	10.8	0.3	11.9	0.5	12.1	0.4
Cr	16.7	7.2	—	—	8.78	0.12	9.14	0.44	7.22	0.22	7.70	1.85	7.94	1.07	7.20	1.99	8.41	1.03	8.58	2.17

Table 3 (continued).
Measurement results for trace elements in ARM-1, ARM-2 and ARM-3 determined by XRF, ICP-OES, ICP-MS and LA-ICP-MS.

| | XRF | | ICP-OES [2] | | ICP-MS [1] | | ICP-MS [2] | | LA-SF-ICP-MS [3] Spot | | LA-SF-ICP-MS [3] Line | | LA-Q-ICP-MS [4] Spot | | LA-Q-ICP-MS [1] Spot | | LA-SF-ICP-MS [1] Spot (Exp.1) | | LA-SF-ICP-MS [1] Spot (Exp.2) | |
| | n = 4 | | n = 4 | | n = 4 | | n = 4 | | n = 45 | | n = 45 | | n = 40 | | n = 20 | | n = 100 | | n = 15 | |
	Values	2s	Values	2s	Values	2s	Values	2s	Values	2s	Values	2s	Values	2s	Values	2s	Values	2s	Values	2s
Co	–	–	–	–	7.61	0.19	7.59	0.40	7.25	0.26	7.58	1.83	7.44	0.36	6.70	0.42	7.76	0.33	7.67	0.22
Ni	9.97	5.63	–	–	14.4	0.6	8.04	0.21	13.2	1.0	14.4	4.8	12.5	1.0	11.0	2.1	13.3	0.8	13.8	0.3
Cu	13.0	5.6	–	–	13.1	0.5	13.3	0.3	12.5	0.1	13.2	2.6	13.2	0.6	13.0	1.1	16.7	0.7	14.2	0.1
Zn	29.1	2.2	32.4	0.7	30.0	0.9	40.7	4.1	40.1	1.0	41.7	10.4	35.6	2.3	31.3	7.3	41.7	2.3	38.9	0.6
Ga	–	–	–	–	17.2	0.4	17.3	0.3	17.7	0.4	18.1	3.2	16.9	6.1	17.2	0.8	18.4	0.7	18.5	0.6
Ge	–	–	–	–	7.30	0.06	–	–	8.24	0.51	8.30	1.28	8.36	0.64	10.8	2.4	9.53	0.98	9.32	1.12
As	–	–	–	–	–	–	–	–	3830	40	3960	680	3440	80	3560	80	4000	160	3890	40
Rb	–	–	–	–	7.10	0.46	7.23	0.22	7.37	0.11	7.80	1.30	7.67	0.39	6.78	0.84	8.09	0.30	8.28	0.31
Sr	21.5	0.9	–	–	18.7	0.6	21.1	0.5	19.7	0.2	19.7	0.2	19.5	0.5	18.1	1.1	19.0	0.6	19.4	0.5
Y	–	–	–	–	7.28	0.13	6.25	0.22	7.54	0.26	7.29	0.90	7.46	0.28	6.43	0.51	6.89	0.30	7.25	0.30
Zr	9.03	1.98	–	–	9.89	0.21	11.0	0.3	12.0	0.4	11.5	1.3	11.6	0.3	10.1	1.4	11.1	0.5	11.5	0.6
Nb	–	–	–	–	11.6	0.2	12.3	0.4	12.4	0.2	13.0	1.0	12.1	0.3	11.3	0.4	12.7	0.4	12.4	0.3
Mo	–	–	–	–	8.92	0.17	–	–	9.14	0.10	9.45	1.85	9.40	0.72	9.73	0.62	10.0	0.5	9.76	0.82
Cd	–	–	–	–	5.29	0.16	–	–	6.29	0.30	6.76	1.48	5.65	0.95	5.20	0.62	6.84	0.59	6.00	0.33
Sn	–	–	–	–	–	–	–	–	10.9	0.2	11.1	1.8	11.6	0.5	14.2	0.7	11.9	0.5	14.1	0.3
Sb	–	–	–	–	10.8	0.2	–	–	13.4	0.2	13.5	2.2	12.3	0.4	13.3	1.0	14.1	0.7	13.7	0.5
Cs	–	–	–	–	7.17	0.14	8.02	0.12	7.22	0.09	7.58	1.17	7.29	0.20	7.28	0.20	7.88	0.27	7.84	0.09
Ba	–	–	28.7	0.7	27.6	1.5	28.7	0.7	28.7	0.2	29.2	1.9	28.3	1.2	26.9	2.3	28.2	1.3	29.2	0.6
La	–	–	–	–	6.65	0.10	6.50	0.21	6.92	0.16	6.99	0.79	6.59	0.19	6.29	0.24	6.51	0.28	6.52	0.12
Ce	–	–	–	–	8.17	0.03	6.43	0.22	8.07	0.09	9.39	1.74	8.04	0.24	7.59	0.35	8.03	0.29	8.07	0.18
Pr	–	–	–	–	6.02	0.06	5.90	0.21	5.81	0.07	5.86	0.10	5.65	0.20	4.99	0.31	5.59	0.20	5.59	0.12
Nd	–	–	–	–	8.16	0.15	7.43	0.37	7.96	0.13	7.86	0.45	7.58	0.53	6.09	1.13	7.58	0.51	7.56	0.18
Sm	–	–	–	–	6.07	0.07	5.81	0.33	6.22	0.12	6.08	0.41	6.02	0.38	5.77	0.99	5.88	0.43	6.11	0.42
Eu	–	–	–	–	5.88	0.05	5.42	0.04	5.98	0.06	5.93	0.22	5.68	0.17	5.43	0.24	5.63	0.25	5.76	0.10
Gd	–	–	–	–	6.37	0.09	5.80	0.13	6.20	0.18	5.93	0.64	6.03	0.42	5.84	0.56	5.79	0.43	6.03	0.28
Tb	–	–	–	–	6.94	0.14	6.94	0.27	7.04	0.18	6.82	0.77	6.57	0.17	6.19	0.21	6.20	0.28	6.25	0.06
Dy	–	–	–	–	6.53	0.06	6.13	0.23	6.54	0.19	6.19	0.83	6.32	0.34	5.67	0.37	6.03	0.33	6.01	0.03
Ho	–	–	–	–	7.25	0.13	7.57	0.32	7.70	0.25	7.33	0.95	7.20	0.22	6.75	0.30	6.73	0.35	6.80	0.25
Er	–	–	–	–	6.45	0.15	6.15	0.32	6.69	0.20	6.30	0.80	6.47	0.28	5.97	0.52	6.01	0.28	6.17	0.21
Tm	–	–	–	–	6.75	0.09	6.42	0.31	6.99	0.24	6.63	0.89	6.53	0.18	6.17	0.10	6.06	0.27	6.23	0.20
Yb	–	–	–	–	8.54	0.06	8.85	0.44	9.63	0.26	9.22	1.04	9.11	0.38	8.20	0.42	8.69	0.54	8.83	0.36
Lu	–	–	–	–	6.34	0.09	6.47	0.40	7.03	0.23	6.71	0.89	6.58	0.25	6.27	0.33	6.15	0.30	6.34	0.09
Hf	–	–	–	–	6.22	0.05	6.37	0.11	6.58	0.27	6.21	0.87	6.20	0.38	5.96	0.59	5.87	0.43	6.31	0.53
Ta	–	–	–	–	5.77	0.11	6.52	0.14	6.64	0.13	6.54	0.45	6.10	0.16	5.53	0.34	6.19	0.31	6.04	0.15
W	–	–	–	–	8.18	0.09	–	–	8.93	0.07	9.15	1.79	8.88	0.42	9.36	0.93	9.50	0.58	9.84	0.44

Table 3 (continued).
Measurement results for trace elements in ARM-1, ARM-2 and ARM-3 determined by XRF, ICP-OES, ICP-MS and LA-ICP-MS

| | XRF [2] | | ICP-OES [2] | | ICP-MS [1] | | ICP-MS [2] | | LA-SF-ICP-MS [3] Spot | | LA-SF-ICP-MS [3] Line | | LA-Q-ICP-MS [4] Spot | | LA-Q-ICP-MS [1] Spot | | LA-SF-ICP-MS [1] Spot (Exp.1) | | LA-SF-ICP-MS [1] Spot (Exp.2) | |
| | n = 4 | | n = 4 | | n = 4 | | n = 4 | | n = 45 | | n = 45 | | n = 40 | | n = 20 | | n = 100 | | n = 15 | |
	Values	2s	Values	2s	Values	2s	Values	2s	Values	2s	Values	2s	Values	2s	Values	2s	Values	2s	Values	2s
Tl	–	–	–	–	–	–	3.10	0.80	3.30	0.10	3.52	0.47	3.24	0.16	3.68	0.21	4.51	0.33	3.62	0.06
Pb	–	–	–	–	11.0	0.2	12.3	0.2	13.0	0.3	13.3	2.1	12.3	0.4	12.6	0.6	13.7	0.5	13.6	0.3
Bi	–	–	–	–	12.3	0.1	–	–	14.6	0.3	13.6	1.8	13.3	0.4	13.4	0.5	15.4	0.7	14.5	0.2
Th	–	–	–	–	3.26	0.06	3.24	0.24	3.55	0.09	3.44	0.34	3.26	0.13	3.07	0.12	3.19	0.16	3.20	0.03
U	–	–	–	–	3.36	0.05	3.70	0.10	3.76	0.03	4.05	0.81	3.73	0.15	3.78	0.37	3.89	0.19	3.70	0.07

Mass fraction data are given in µg g^{-1}. ICP-OES[2] represents ICP-OES at NRCG. ICP-MS[1] represents ICP-OES at NRCG. ICP-MS[2] represents ICP-MS at IGGCAS. ICP-MS[3] represents ICP-MS at IGGCAS. LA-SF-ICP-MS[3] represents the data from IGGCAS. LA-SF-ICP-MS[1] represents the data from CUG. LA-Q-ICP-MS[1] represents the data from IGGCAS. LA-Q-ICP-MS[4] represents the data from MPI. LA-Q-ICP-MS[4] represents the

although quite different techniques were applied. Nearly, all the lithophile elements are in agreement within ± 15%. The poor agreement observed for some chalcophile/siderophile elements (Cu, Zn, Ni and Tl) may be attributed to their low abundances (Tl in ARM-2) and/or analytical limitations. The solution ICP-MS data are in agreement with the LA-ICP-MS results (Figure 6), also demonstrating the good quality of LA-ICP-MS analytical measurements.

Preliminary reference values

The three ARM glasses were made to provide new reference materials for geochemical, microanalytical *in situ* techniques, in particular for LA-ICP-MS. It is desirable that these glasses should comply with the ISO definition of a reference material, namely a 'material or substance one or more of whose property values are sufficiently homogeneous and well established to be used for the calibration of an apparatus, the assessment of a measurement method, or for assigning values to materials' (ISO Guide 30, 1992). However, the number of analytical data presented here is still insufficient for a certification procedure defined by ISO Guide 35. Therefore, we follow the IAG recommendations to determine preliminary reference values for the ARM glasses. Traceability is a key concept in the characterisation of reference materials. In this study, the traceability of the quality of our analytical results was established by the use of international reference materials for calibrations and by using various analytical techniques. NIST SRM 610 was used as the calibration material and Ca as the internal standard for all LA-ICP-MS analyses; thus, our LA-ICP-MS data are traceable to the well-characterised NIST SRM 610. All chemical data are reported here with analytical uncertainties. The collaborating laboratories have previously demonstrated their analytical competence using well-established methods. Therefore, the results of analytical data presented here for the ARM glasses are robust and the averaged analytical results from different laboratories using independent techniques can be considered reliable preliminary reference values for the ARM glasses. Statistical outliers were excluded as they are probably caused by technical problems during analysis or are due to calibration errors. Results listed in Table 4 are classified into two categories: preliminary reference values and information values. Preliminary reference values are reported when data obtained from at least three laboratories using three or more independent, well-defined techniques were in statistical agreement. Their quoted uncertainties are defined as two times the standard error (2SE, standard deviation of the mean of *n* contributing laboratory mean data). Information values with a standard deviation of the mean are derived from the data of at least two laboratories using two

Table 4.
Preliminary values (in bold) and information values for ARM-1, ARM-2 and ARM-3

	ARM-1				ARM-2				ARM-3			
	Values	2SE	2RSE (%)	n	Values	2SE	2RSE (%)	n	Values	2SE	2RSE (%)	n
SiO_2	**58.4**	**0.5**	**0.8**	2	**57.9**	**0.5**	**0.8**	2	**60.3**	**0.08**	**0.2**	2
TiO_2	**0.98**	**0.03**	**2.8**	4	**0.97**	**0.04**	**4.2**	4	**1.01**	**0.03**	**3.2**	4
Al_2O_3	**13.3**	**0.1**	**0.5**	4	**13.1**	**0.1**	**0.9**	4	**13.8**	**0.1**	**0.2**	4
FeO_t	**5.72**	**0.10**	**1.4**	4	**5.72**	**0.10**	**1.3**	4	**5.91**	**0.09**	**1.5**	4
MnO	**0.04**	**0.01**	**29.4**	4	**0.05**	**0.01**	**7.1**	4	**0.05**	**0.01**	**3.5**	4
MgO	**3.78**	**0.11**	**2.9**	4	**3.74**	**0.10**	**2.8**	4	**3.51**	**0.08**	**2.2**	4
CaO	**5.07**	**0.06**	**0.9**	4	**5.01**	**0.07**	**1.4**	4	**5.32**	**0.04**	**0.8**	4
Na_2O	**4.43**	**0.04**	**0.9**	4	**4.42**	**0.05**	**1.1**	4	**4.66**	**0.05**	**1.0**	4
K_2O	**3.13**	**0.02**	**0.6**	4	**3.00**	**0.05**	**1.7**	4	**3.18**	**0.04**	**1.2**	4
P_2O_5	**0.26**	**0.01**	**3.6**	3	**0.29**	**0.01**	**5.0**	3	**0.27**	**0.02**	**8.3**	3
Li	511	21	4.1	8	1230	62	5.0	8	18.6	1.0	5.2	8
Be	475	22	4.6	8	54.7	1.5	2.8	8	6.29	0.34	5.4	8
B	463	52	11.2	8	10500	770	7.4	8	60.6	3.7	6.0	8
Sc	428	42	9.8	8	51.5	1.2	2.3	8	7.02	0.36	5.1	8
V	**575**	**19**	**3.3**	8	**55.8**	**2.0**	**3.6**	8	**12.2**	**1.1**	**8.9**	8
Cr	**463**	**38**	**8.3**	9	**61.0**	**6.1**	**10.1**	9	**9.07**	**1.85**	**20.4**	9
Co	497	9	1.8	8	**59.6**	**0.7**	**1.2**	8	7.45	0.22	3.0	8
Ni	**473**	**17**	**3.7**	9	**59.2**	**1.9**	**3.3**	9	**12.3**	**1.4**	**11.2**	9
Cu	446	19	4.2	9	55.6	3.1	5.5	9	13.6	0.8	5.8	9
Zn	**558**	**27**	**4.9**	10	**5120**	**290**	**5.6**	10	**36.1**	**3.1**	**8.4**	10
Ga	489	23	4.8	8	69.9	2.9	4.1	8	17.7	0.4	2.3	8
Ge	626	32	5.2	7	68.3	4.7	6.9	7	8.84	0.79	9.0	7
As	3360	181	5.4	6	3480	140	4.1	6	3780	170	4.5	6
Rb	486	21	4.3	8	57.6	2.7	4.6	8	7.54	0.34	4.5	8
Sr	**465**	**7**	**1.6**	9	**64.2**	**1.3**	**2.1**	9	**19.6**	**0.7**	**3.4**	9
Y	449	16	3.7	8	51.1	1.0	2.0	8	7.05	0.32	4.5	8
Zr	**437**	**10**	**2.3**	9	**56.8**	**2.2**	**3.9**	9	**10.9**	**0.6**	**5.6**	9
Nb	471	14	2.9	8	57.7	1.4	2.5	8	12.2	0.4	3.1	8
Mo	486	17	3.6	7	57.2	2.3	4.0	7	9.49	0.27	2.9	7
Cd	463	20	4.3	7	50.2	2.2	4.3	7	6.00	0.46	7.7	7
Sn	592	25	4.2	6	72.8	2.8	3.8	6	**12.3**	**1.1**	8.9	6
Sb	533	29	5.4	7	62.6	3.7	5.8	7	13.0	0.8	6.0	7
Cs	474	19	3.9	8	51.9	1.7	3.4	8	7.53	0.22	3.0	8
Ba	**2030**	**53**	**2.6**	10	**249**	**5**	**1.9**	10	**28.4**	**0.5**	**1.6**	10
La	452	11	2.4	8	52.0	1.1	2.1	8	6.62	0.15	2.3	8
Ce	444	14	3.2	8	53.7	0.9	1.6	8	7.97	0.54	6.7	8
Pr	430	18	4.2	8	49.8	1.6	3.2	8	5.68	0.21	3.7	8
Nd	440	16	3.7	8	55.5	1.4	2.5	8	7.53	0.42	5.5	8
Sm	462	13	2.9	8	51.6	1.0	1.9	8	6.00	0.10	1.8	8
Eu	457	12	2.7	8	50.7	0.7	1.4	8	5.71	0.14	2.5	8
Gd	446	13	3.0	8	48.9	0.8	1.7	8	6.00	0.14	2.3	8
Tb	435	18	4.1	8	49.0	1.8	3.8	8	6.62	0.24	3.6	8
Dy	453	13	3.0	8	53.6	1.3	2.5	8	6.18	0.19	3.1	8
Ho	450	18	4.1	8	50.6	2.1	4.2	8	7.17	0.25	3.5	8
Er	461	10	2.2	8	52.8	1.0	1.8	8	6.28	0.16	2.6	8
Tm	423	15	3.6	8	49.5	1.4	2.9	8	6.47	0.21	3.2	8
Yb	460	11	2.4	8	669	10	1.5	8	8.88	0.29	3.3	8
Lu	446	13	2.9	8	48.6	1.5	3.0	8	6.48	0.19	2.9	8
Hf	457	16	3.5	8	51.5	1.0	2.0	8	6.21	0.15	2.4	8
Ta	454	14	3.2	8	51.2	1.8	3.5	8	6.16	0.26	4.2	8
W	454	23	5.2	7	55.9	2.3	4.1	7	9.12	0.37	4.1	7
Tl	35.0	4	10.9	6	0.14	0.07	49.6	6	3.57	0.35	9.9	6
Pb	614	34	5.5	8	76.2	3.4	4.4	8	12.7	0.6	4.6	8
Bi	591	40	6.8	7	69.9	3.7	5.4	7	13.9	0.7	5.2	7
Th	12.4	0.3	2.1	7	13.1	0.3	2.6	7	3.28	0.11	3.3	7
U	12.5	0.5	3.9	8	13.4	0.4	3.1	8	3.75	0.13	3.5	8

Major and trace element mass fractions are given in % m/m and $\mu g\ g^{-1}$, respectively. The quoted uncertainties are defined as two times the standard error (2SE, standard deviation of the mean of n contributing laboratory mean data).

independent techniques. All other results from only one single laboratory or analytical technique are listed as information values without standard deviations.

Further characterisation with different *in situ* and bulk techniques (e.g., SIMS, LA-MC-ICP-MS, ID-ICP-MS, ID-TIMS, ID-MC-ICP-MS) is underway in approximately fifty laboratories. We are confident that based on this characterisation, the three ARM glasses may be established as new reference materials for *in situ* techniques, as a complement and alternative to widely used NIST and USGS GS glasses for LA-(MC)-ICP-MS analysis in the near future. High Li-B contents ($\sim$ 1000 µg g^{-1} for Li and $\sim$ 10000 µg g^{-1} for B) of ARM-2 make this glass potentially suitable also for *in situ* Li-B isotope reference material.

Conclusions

In this study, we prepared and preliminarily characterised three new synthetic andesite reference glasses for microanalytical work, in particular for LA-ICP-MS. These andesitic glasses ('Andesite Reference Glass Materials': ARM-1, 2 and 3) contain fifty-four trace elements with nearly identical abundance ($\sim$ 500, $\sim$ 50, $\sim$ 5 µg g^{-1}). Micro- and bulk analyses indicate that the glasses are well homogenised with respect to major and trace elements. Discrepancies in the data for V, Cr, Ni and Tl exist, which are mainly caused by analytical limitations. Based on the new analytical data, preliminary reference and information values for fifty-six elements were presented. The analytical uncertainties [2 relative standard error (RSE)] were estimated to be in the range of 1–20%. The three ARM glasses (after a further certification project) should become new certified reference materials for *in situ* techniques, in particular for LA-ICP-MS.

We further document an acquisition method for SF-ICP-MS (Element 2 and Element XR), which is capable of sweeping seventy-seven isotopes (sixty-eight elements) from ^{7}Li to ^{238}U in 1 s. The stability and accuracy were confirmed by analysing several well-characterised reference glasses. We also report the results of USGS NKT-1G and TB-1G using LA-SF-ICP-MS. The values of these two reference glasses have been rarely reported, and our data may be useful for certification procedures.

Acknowledgements

Availability of ARM glasses

We are willing to distribute appropriate but limited amounts of the ARM glasses to the scientific community on request (S.-T Wu, e-mail: shitou.wu@mail.iggcas.ac.cn).

References

Eggins S.M., Rudnick R.L. and McDonough W.F. (1998)
The composition of peridotites and their minerals: A laser-ablation ICP-MS study. Earth and Planetary Science Letters, 154, 53–71.

Elburg M., Vroon P., van der Wagt B. and Tchalikian A. (2005)
Sr and Pb isotopic composition of five USGS glasses (BHVO-2G, BIR-1G, BCR-2G, TB-1G, NKT-1G). Chemical Geology, 223, 196–207.

Flem B., Larsen R.B., Grimstvedt A. and Mansfeld J. (2002)
In situ analysis of trace elements in quartz by using laser ablation inductively coupled plasma-mass spectrometry. Chemical Geology, 182, 237–247.

Fryer B.J., Jackson S.E. and Longerich H.P. (1995)
The design, operation and role of the laser-ablation microprobe coupled with an inductively coupled plasma-mass spectrometer (LAM-ICP-MS) in the Earth sciences. Canadian Mineralogist, 33, 303–312.

Gao S., Liu X.M., Yuan H.L., Hattendorf B., Günther D., Chen L. and Hu S.H. (2002)
Determination of forty-two major and trace elements in USGS and NIST SRM glasses by laser ablation-inductively coupled plasma-mass spectrometry. Geostandards Newsletter: The Journal of Geostandards and Geoanalysis, 26, 181–196.

Garbe-Schönberg D. and Müller S. (2014)
Nano-particulate pressed powder tablets for LA-ICP-MS. Journal of Analytical Atomic Spectrometry, 29, 990–1000.

Gray A.L. (1985)
Solid sample introduction by laser ablation for inductively coupled plasma source mass spectrometry. Analyst, 110, 551–556.

Guillong M., Horn I. and Günther D. (2003)
A comparison of 266 nm, 213 nm and 193 nm produced from a single solid state Nd:YAG laser for laser ablation ICP-MS. Journal of Analytical Atomic Spectrometry, 18, 1224–1230.

Harries D. (2014)
Homogeneity testing of microanalytical reference materials by electron probe microanalysis (EPMA). Chemie der Erde-Geochemistry, 74, 375–384.

references

He Z., Huang F., Yu H., Xiao Y., Wang F., Li Q., Xia Y. and Zhang X. (2016)
A flux-free fusion technique for rapid determination of major and trace elements in silicate rocks by LA-ICP-MS. Geostandards and Geoanalytical Research, 40, 5–21.

Hofmann A. (2003)
Sampling mantle heterogeneity through oceanic basalts: Isotopes and trace elements. Treatise on Geochemistry, 2, 568.

ISO Guide 30 (1992)
Terms and definitions used in connection with reference materials (2nd edition). International Organization for Standardization (Geneva), 8pp.

Jackson S.E., Longerich H.P., Dunning G.R. and Fryer B.J. (1992)
The application of laser-ablation microprobe-inductively coupled plasma-mass spectrometry (LAM-ICP-MS) to in situ trace-element determinations in minerals. The Canadian Mineralogist, 30, 1049–1064.

Jeffries T.E., Jackson S.E. and Longerich H.P. (1998)
Application of a frequency quintupled Nd: YAG source (λ = 213 nm) for laser ablation inductively coupled plasma-mass spectrometric analysis of minerals. Journal of Analytical Atomic Spectrometry, 13, 935–940.

Jenner F.E. and O'Neill H.S.C. (2012)
Major and trace analysis of basaltic glasses by laser-ablation ICP-MS. Geochemistry, Geophysics, Geosystems, 13, 1–17.

Jenner G.A., Longerich H.P., Jackson S.E. and Fryer B.J. (1990)
ICP-MS – A powerful tool for high-precision trace-element analysis in Earth sciences: Evidence from analysis of selected U.S.G.S. reference samples. Chemical Geology, 83, 133–148.

Jochum K.P. and Enzweiler J. (2014)
Reference materials in geochemical and environmental research. Treatise on Geochemistry (2nd edition). Elsevier (Oxford), 43–70.

Jochum K.P., Dingwell D.B., Rocholl A., Stoll B., Hofmann A.W., Becker S., Besmehn A., Bessette D., Dietze H.J. and Dulski P. (2000)
The preparation and preliminary characterisation of eight geological MPI-DING reference glasses for in situ microanalysis. Geostandards Newsletter: The Journal of Geostandards and Geoanalysis, 24, 87–133.

Jochum K.P., Willbold M., Raczek I., Stoll B. and Herwig K. (2005)
Chemical characterisation of the USGS reference glasses GSA-1G, GSC-1G, GSD-1G, GSE-1G, BCR-2G, BHVO-2G and BIR-1G using EPMA, ID-TIMS, ID-ICP-MS and LA-ICP-MS. Geostandards and Geoanalytical Research, 29, 285–302.

Jochum K.P., Stoll B., Herwig K., Willbold M., Hofmann A.W., Amini M., Aarburg S., Abouchami W., Hellebrand E., Mocek B., Raczek I., Stracke A., Alard O., Bouman C., Becker S., Dücking M., Brätz H., Klemd R., de Bruin D., Canil D., Cornell D., de Hoog C.-J., Dalpé C., Danyushevsky L., Eisenhauer A., Gao Y., Snow J.E., Groschopf
N., Günther D., Latkoczy C., Guillong M., Hauri E.H., Höfer H.E., Lahaye Y., Horz K., Jacob D.E., Kasemann S.A., Kent A.J.R., Ludwig T., Zack T., Mason P.R.D., Meixner A., Rosner M., Misawa K., Nash B.P., Pfänder J., Premo W.R., Sun W.D., Tiepolo M., Vannucci R., Vennemann T., Wayne D. and Woodhead J.D. (2006)
MPI-DING reference glasses for in situ microanalysis: New reference values for element concentrations and isotope ratios. Geochemistry, Geophysics, Geosystems, 7, 1–44.

Jochum K.P., Stoll B., Herwig K. and Willbold M. (2007)
Validation of LA-ICP-MS trace element analysis of geological glasses using a new solid-state 193 nm Nd:YAG laser and matrix-matched calibration. Journal of Analytical Atomic Spectrometry, 22, 112–121.

Jochum K.P., Scholz D., Stoll B., Weis U., Wilson S.A., Yang Q.C., Schwalb A., Borner N., Jacob D.E. and Andreae M.O. (2012)
Accurate trace element analysis of speleothems and biogenic calcium carbonate by LA-ICP-MS. Chemical Geology, 318, 31–44.

Jochum K.P., Stoll B., Weis U., Jacob D.E., Mertz-Kraus R. and Andreae M.O. (2014)
Non-matrix-matched calibration for the multi-element analysis of geological and environmental samples using 200 nm femtosecond LA-ICP-MS: A comparison with nanosecond lasers. Geostandards and Geoanalytical Research, 38, 265–292.

Kimura J.-I. and Chang Q. (2012)
Origin of the suppressed matrix effect for improved analytical performance in determination of major and trace elements in anhydrous silicate samples using 200 nm femtosecond laser ablation sector-field inductively coupled plasma-mass spectrometry. Journal of Analytical Atomic Spectrometry, 27, 1549–1559.

Latkoczy C. and Günther D. (2002)
Enhanced sensitivity in inductively coupled plasma sector field mass spectrometry for direct solid analysis using laser ablation (LA-ICP-SFMS). Journal of Analytical Atomic Spectrometry, 17, 1264–1270.

Liu Y.S., Hu Z.C., Gao S., Günther D., Xu J., Gao C.G. and Chen H.H. (2008)
In situ analysis of major and trace elements of anhydrous minerals by LA-ICP-MS without applying an internal standard. Chemical Geology, 257, 34–43.

Ødegård M. and Hamester M. (1997)
Preliminary investigation into the use of a high resolution inductively coupled plasma-mass spectrometer with laser ablation for bulk analysis of geological materials fused with $Li_2B_4O_7$. Geostandards Newsletter: The Journal of Geostandards and Geoanalysis, 21, 245–252.

Peters D. and Pettke T. (2017)
Evaluation of major to ultra trace element bulk rock chemical analysis of nanoparticulate pressed powder pellets by LA-ICP-MS. Geostandards and Geoanalytical Research, 41, 5–28.

references

Raczek I., Stoll B., Hofmann A.W. and Jochum K.P. (2001)
High-precision trace element data for the USGS reference materials BCR-1, BCR-2, BHVO-1, BHVO-2, AGV-1, AGV-2, DTS-1, DTS-2, GSP-1 and GSP-2 by ID-TIMS and MIC-SSMS. Geostandards Newsletter: The Journal of Geostandards and Geoanalysis, 25, 77–86.

Regnery J., Stoll B. and Jochum K.P. (2010)
High-resolution LA-ICP-MS for accurate determination of low abundances of K, Sc and other trace elements in geological samples. Geostandards and Geoanalytical Research, 34, 19–38.

Rudnick R. and Gao S. (2003)
Composition of the continental crust. Treatise on Geochemistry, 3, 1–64.

Sylvester P.J. and Jackson S.E. (2016)
A brief history of laser ablation inductively coupled plasma-mass spectrometry (LA-ICP-MS). Elements, 12, 307–310.

Tiepolo M., Bottazzi P., Palenzona M. and Vannucci R. (2003)
A laser probe coupled with ICP-double-focusing sector-field mass spectrometer for in situ analysis of geological samples and U-Pb dating of zircon. The Canadian Mineralogist, 41, 259–272.

Walle M. and Heinrich C.A. (2014)
Fluid inclusion measurements by laser ablation sector-field ICP-MS. Journal of Analytical Atomic Spectrometry, 29, 1052–1057.

Willbold M., Jochum K.P., Raczek I., Amini M.A., Stoll B. and Hofmann A.W. (2003)
Validation of multi-element isotope dilution ICP-MS for the analysis of basalts. Analytical and Bioanalytical Chemistry, 377, 117–125.

Wu S., Wang Y., Sun D., Wen H., Xu C. and Wang W. (2014)
Determination of 15 rare earth elements in rare earth ores by inductively coupled plasma-atomic emission spectrometry: A comparison of four different pretreatment methods. Rock and Mineral Analysis, 33, 12–19. (in Chinese with English abstract)

Wu C.-C., Burger M., Günther D., Shen C.-C. and Hattendorf B. (2018a)
Highly-sensitive open-cell LA-ICP-MS approaches for the quantification of rare earth elements in natural carbonates at parts-per-billion levels. Analytica Chimica Acta, 1018, 54–61.

Wu S., Karius V., Schmidt B.C., Simon K. and Wörner G. (2018b)
Comparison of ultrafine powder pellet and flux-free fusion glass for bulk analysis of granitoids by laser ablation-inductively coupled plasma-mass spectrometry. Geostandards and Geoanalytical Research, 42, 575–591.

Supporting information

The following supporting information may be found in the online version of this article:

Appendix S1. Tables S1–3: Oxide chemicals used for ARM glasses; acquisition list parameters of sector field ICP-MS; reference values of NIST SRM 610, MPI-DING StHs6/80-G and USGS GSD-1G.

Appendix S2. Information on all instrument operating parameters for this study.

Appendix S3. Figures S1–S4: Measurement repeatability and intermediate measurement precision of laser ablation sector-field ICP-MS on MPI-DING StHs6/80-G; Rare earth patterns normalised to Chondrite C1 for TI-G and BCR-2G and CGSG-4; Comparison of the results of NIST SRM 612, ML3B-G and BCR-2G obtained from GZG and IGGCAS; Relative standard deviation (%) of multiple spot analyses for ARM glasses.

This material is available from: http://onlinelibrary.wiley.com/doi/10.1111/ggr.12301/abstract (This link will take you to the article abstract).